MEMBRANE VISCOPLASTIC FLOW

E. A. EVANS *and* R. M. HOCHMUTH

From the Departments of Biomedical Engineering and Surgery, Duke University, Durham, North Carolina 27706, and the Department of Chemical Engineering, Washington University, St. Louis, Missouri 63130. Dr. Hochmuth's present address is the Department of Biomedical Engineering, Duke University.

ABSTRACT In this paper, a theory of viscoplasticity formulated by Prager and Hohenemser is developed for a two-dimensional membrane surface and applied to the analysis of the flow of "microtethers" pulled from red blood cells attached to glass substrates. The viscoplastic flow involves two intrinsic material constants: yield shear and surface viscosity. The intrinsic viscosity for plastic flow of membrane is calculated to be 1×10^{-2} dyn-s/cm from microtether flow experiments, *three orders* of magnitude *greater* than surface viscosities of lipid membrane components. The fluid dissipation is dominated by the flow of a structural matrix which has exceeded its yield shear. The yield shear is the maximum shear resultant that the membrane can sustain before it begins to deform irreversibly. The yield shear is found to be in the range $2\text{–}8 \times 10^{-2}$ dyn/cm, *two* or *three* orders of magnitude *smaller* than the isotropic tension required to lyse red cells.

INTRODUCTION

The material structure of a plasma membrane determines the viability of the membrane when exposed to external forces. In turn, the security of the cell cytoplasm and the life of the cell are dependent on the integrity of the membrane. Because of the importance of the strength of the membrane, considerable research has been undertaken to determine the "deformability" and elasticity of plasma membranes. Most of these experiments have been performed on the human red blood cell because of its geometric simplicity and essentially homogeneous liquid interior surrounded by a plasma membrane. Recently, an innovative, two-dimensional hyperelastic material concept and finite deformation analysis (Skalak et al., 1973; Evans, 1973*a*, *b*) have provided correlation of existing elasticity experiments on fluid shear and micropipette deformation of human red cells (Hochmuth and Mohandas, 1972; Evans, 1973*b*; Evans and LaCelle, 1975).

Although the *solid* property of elasticity has been studied both experimentally and theoretically, the irrecoverable, plastic flow of plasma membrane has not been investigated in detail. However, there have been observations of plastic flow and failure of red cell membrane both in in vitro and in vivo (Kochen, 1968; LaCelle, 1970; Bessis, 1973; Weed and Reed, 1965; Bull and Kuhn, 1970; Bull et al., 1968). In particular, Hochmuth et al. (1973) and Williamson et al. (1975) measured the plastic growth of "microtethers" pulled from point attached red cells under the action of fluid shear

stress. *Quantitative* experimental *and* analytical studies of the yield, growth and failure of the membrane material are of interest not only from the scientific viewpoint of material structure but also from the clinical viewpoint concerning membrane failure in hemolytic anemias.

To characterize the *plasticity* of living membrane, both the yield shear and the rate of deformation (related to the intrinsic viscosity) produced by the action of a known membrane shear, must be measured. Fluid-like behavior of lipid bilayers and plasma membranes has been reported in numerous publications (for a review of the relevant literature see Edidin, 1974 *a*, *b*), and the observation of this "fluidity" has stimulated the proposition of a model for membrane structure, the "fluid mosaic model" (Singer and Nicholson, 1972). However, this "fluidity" represents the translational mobility of portions of membrane, or particles located in the lipid bilayer component of the membrane. Mechanical experiments cited above on red cell membranes have demonstrated that an elastic structural component must exist in conjunction with the liquid, lipid bilayer in order to provide the observed membrane elasticity or solid-like behavior. Therefore, a composite arrangement is indicated, conceptually consisting of a two-dimensional structural component covered by a two-dimensional, liquid lipid bilayer (Evans and LaCelle, 1975, and Evans, 1975). The intrinsic viscosity for the plastic flow of membrane includes the effects of frictional dissipation in the structural component responsible for the membrane elasticity as well as that in the liquid, lipid bilayer. Most likely, the frictional dissipation in the structural component will dominate and the viscosity will be primarily indicative of the plastic flow of this component. Obviously, the yield shear of the membrane will only relate to plastic failure of the elastic structural component. Measuring the yield shear and viscosity in plastic flow will, therefore, provide necessary additional information about the membrane composite.

In this communication, a theory of viscoplasticity formulated by Prager and Hohenemser in 1932 (see Prager, 1961) will be developed for a two-dimensional membrane surface (isotropic in the plane of the membrane). Application of this development to microtether growth experiments of Hochmuth et al. (1973) will be considered.

TWO-DIMENSIONAL VISCOPLASTICITY

The fundamental difference between a solid and liquid material is that a solid can sustain a non-zero shear stress without flowing while a liquid cannot. The transition from solid to liquid-like behavior is characterized by a yield stress. For a stress greater than the yield stress, plastic (permanent) deformation occurs with the net shear stress above the yield stress being balanced by the viscous dissipation which results from the flow of the material. The simple theory of viscoplasticity introduced by Bingham in 1922 and generalized by Hohenemser and Prager in 1932 (see Prager, 1961) involves two intrinsic material constants: a yield stress and a viscosity. Here, we will adapt the theory to the flow of a two-dimensional membrane material. (It is important to recognize that viscous dissipation also occurs during the elastic deformation of the membrane. In general, the viscosity parameter that characterizes the viscoelastic response will be

different than the plastic flow constant. In a companion article, a simple viscoelastic resultant vs. finite deformation and rate of deformation constitutive relation is presented and a relaxation experiment is analyzed to obtain the viscosity parameter.)

As previously mentioned, the membrane behaves as a two-dimensional anisotropic material (Evans, 1973 *a*, *b*; Skalak et al., 1973). Stresses in the plane of the membrane are not coupled to the direction normal to the surface,[1] i.e., the membrane cannot change thickness in response to an in-plane stress but can only change surface geometry. From the viewpoint of ultrastructure, this is expected because the material is a composite of molecular monolayers: a continuum in two-dimensions with a molecular character in the third. Because of the fixed thickness, an applied force is considered to be distributed per unit length (resultants) on the side of a surface element in contrast to the stress concept of force per unit area. In addition, the red cell membrane exhibits both elastic (solid) and viscous (fluid-like) behavior (Hochmuth et al., 1973). Therefore, the simplest constitutive equation which describes the *plastic* behavior of this membrane will have a *yield shear* (with CGS units of dynes per centimeter) and *surface viscosity* (dyn-s/cm) as material constants in a *tensor* relationship between membrane resultants and rate of deformation. In this case, the rate of deformation will be proportional to the resultant deviator and a yield function (Prager, 1961):

$$2\eta_p V_{ij} = \begin{cases} 0; & F < 0 \\ FT'_{ij}; & F \geq 0 \end{cases} \tag{1}$$

where η_p is the membrane (surface) viscosity in plastic flow, V_{ij} is the rate of deformation tensor in the plane of the membrane (the indices i, j represent the in-plane membrane coordinates, either 1 or 2), F is the yield function (when $F < 0$, the membrane behaves in a rigid, solid manner; when $F \geq 0$, the membrane flows with a non-zero rate of deformation) and T'_{ij} is the resultant deviator. The resultant deviator is the difference between the resultant tensor (describing the force distribution in the membrane) and the mean tension in the membrane:

$$T'_{ij} = T_{ij} - \tfrac{1}{2} T_{kk} \delta_{ij}, \tag{2}$$

where δ_{ij} is the identity matrix. (The Einstein summation convention for repeated indices will be used). The resultant deviator is zero when the shear resultant in the membrane is zero. The membrane is assumed to be isotropic in the plane of the surface (on the scale of the two-dimensional continuum). Therefore, the yield function will depend only on the second invariant, T'_{II}, of the resultant deviator (the first invariant is the trace, which is identically zero, $T'_{kk} \equiv 0$). The simple relationship for the yield function proposed by Hohenemser and Prager (see Prager, 1961) for three-dimensional materials can be expressed for the membrane as,

$$F = 1 - (T_0 / |T'_{II}|^{1/2}), \tag{3}$$

[1] Hydrostatic pressure differences must be opposed by resultant components that arise from surface curvature.

where T_0 is the yield shear. The second invariant of the resultant deviator is given by

$$T'_{II} = T'^2_{12} - T'_{11}T'_{22}, \tag{4}$$

which is the square of the *maximum shear resultant* in the material element. If the maximum shear resultant is less than the yield shear, then the yield function is negative and, by definition, the rate of deformation tensor is zero. Elastic, recoverable deformation will take place.

The rate of deformation tensor V_{ij} is determined by the time rate of change of the Lagrangian strain tensor. The Lagrangian strain tensor is defined by the change in the square of the metric length in the instantaneous coordinate system (ds^2) relative to that in the initial material coordinate system (ds_0^2):

$$ds^2 - ds_0^2 = dx_k dx_k - da_k da_k = 2\epsilon_{ij} da_i da_j, \tag{5}$$

where dx_k is the kth component of the length element in the instantaneous state and da_k is the kth component of the length element in the initial state. From the chain rule, the Lagrangian strain tensor, ϵ_{ij}, is given by

$$\epsilon_{ij} = \tfrac{1}{2}\left[(\partial x_k/\partial a_i)(\partial x_k/\partial a_j) - \delta_{ij}\right]. \tag{6}$$

By taking the material rate of change of Eq. 5, the rate of deformation tensor is obtained in terms of the time rate of change of the Lagrangian strain tensor:

$$\left[(\partial v_i/\partial x_j) + (\partial v_j/\partial x_i)\right] dx_i dx_j = 2\dot{\epsilon}_{ij} da_i da_j, \tag{7}$$

where $(\dot{})$ denotes the partial derivative with respect to time; v_i is the ith component of the in-plane velocity field, $\dot{x}_i$. The rate of deformation tensor is

$$V_{ij} = \tfrac{1}{2}\left[(\partial v_i/\partial x_j) + (\partial v_j/\partial x_i)\right]. \tag{8}$$

For an arbitrary choice of vectors, Eq. 7 becomes,

$$V_{ij} = \dot{\epsilon}_{kl}(\partial a_k/\partial x_i)(\partial a_l/\partial x_j). \tag{9}$$

Fig. 1 illustrates the deformation of a membrane element in the principal axis coordinate system. The derivatives, dx_1/da_1 and dx_2/da_2, define the principal extension ratios of the material axis, λ_1 and λ_2. (The element has been deformed from the natural or force free state to the elastic limit, determined by the yield shear T_0. This must be taken into account when considering the overall growth of the element from the natural state.) The principal strains are

$$\epsilon_{11} = (\lambda_1^2 - 1)/2, \qquad \epsilon_{22} = (\lambda_2^2 - 1)/2,$$
$$\lambda_1 = dx_1/da_1, \qquad \lambda_2 = dx_2/da_2. \tag{10}$$

Using Eq. 9, the rate of deformation tensor components can be determined:

$$V_{11} = \dot{\lambda}_1/\lambda_1 = \partial v_1/\partial x_1$$
$$V_{22} = \dot{\lambda}_2/\lambda_2 = \partial v_2/\partial x_2$$
$$V_{12} = V_{21} = 0. \tag{11}$$

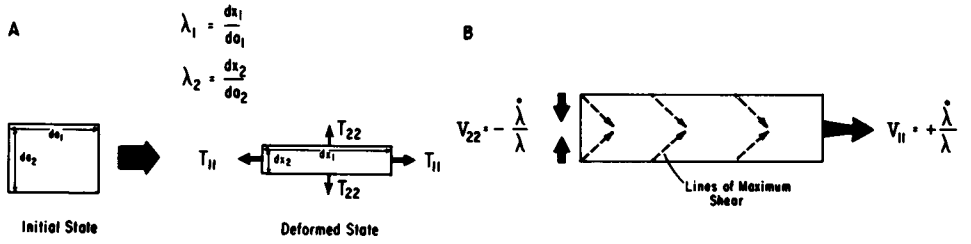

FIGURE 1 Schematic illustration of (*A*) the deformation of a square membrane material element in the principal axis system and (*B*) the principal components of the rate of deformation of the plane element in extension. The principal tensions, T_{11} and T_{22}, are forces per unit length. (Fig. from Evans and Hochmuth, 1976.)

(The principal axis system orientation is assumed not to change with time.) The condition of two-dimensional incompressibility (constant element area) is defined by $\lambda_1 \cdot \lambda_2 = 1$. Therefore, the time rate of change of the extension ratio in one direction is simply related to the time rate of change of the other extension ratio.

$$\dot{\lambda}_2/\lambda_2 = -\dot{\lambda}_1/\lambda_1 \tag{12}$$

and

$$V_{22} = -V_{11}.$$

In Eulerian variables, the two-dimensional incompressibility condition is given by

$$(\partial v_1/\partial x_1) + (\partial v_2/\partial x_2) = 0.$$

The resultant deviator in the principal axis system is,

$$\begin{aligned} T'_{11} &= (T_{11}/2) - (T_{22}/2), \\ T'_{22} &= -(T_{11}/2) + (T_{22}/2), \\ T'_{12} &= T'_{21} = 0, \end{aligned} \tag{13}$$

and the second invariant of the resultant deviator is (from Eq. 4) the square of the maximum shear resultant

$$T'_{II} = [(T_{11}/2) - (T_{22}/2)]^2. \tag{14}$$

Eqs. 11, 13, 14 create a single viscoplastic flow relation from Eq. 1

$$2\eta_p(\dot{\lambda}_1/\lambda_1) = \begin{cases} 0; F < 0. \\ (T_{11}/2) - (T_{22}/2) - T_0; F \geq 0 \end{cases} \tag{15}$$

where the yield function is

$$F = 1 - T_0/|(T_{11}/2) - (T_{22}/2)|.$$

The viscoplastic flow relation (15) can be expressed in Eulerian variables as

$$2\eta_p(\partial v_1/\partial x_1) = \begin{cases} 0; F < 0 \\ (T_{11}/2) - (T_{22}/2) - T_0; F \geq 0 \end{cases} \quad (16)$$

Eq. 15 relates the time rate of plastic growth of the element to the applied membrane tension. Eq. 16 relates the velocity gradient to the applied membrane tension. The former is useful when considering the change in shape of a specific element as time progresses; the latter facilitates the solution of membrane flow behavior in a fixed (Eulerian) frame of reference.

PLASTIC GROWTH OF A MICROTETHER

Fig. 2 shows a scanning electron micrograph of a glutaraldehyde "fixed" microtether produced by fluid shear of a point attached red blood cell. The main body of the cell is elastically deformed into a teardrop shape and can recover its original discoid geometry (Hochmuth and Mohandas, 1972). The microtether, on the other hand, includes both elastic and plastic deformations; the elastic component is recovered when flow is terminated but the plastic growth is irrecoverable. Because of the limit of optical resolution, the cross-sectional dimensions of the microtether are unobservable during growth; therefore, analysis of the microtether growth is impossible unless

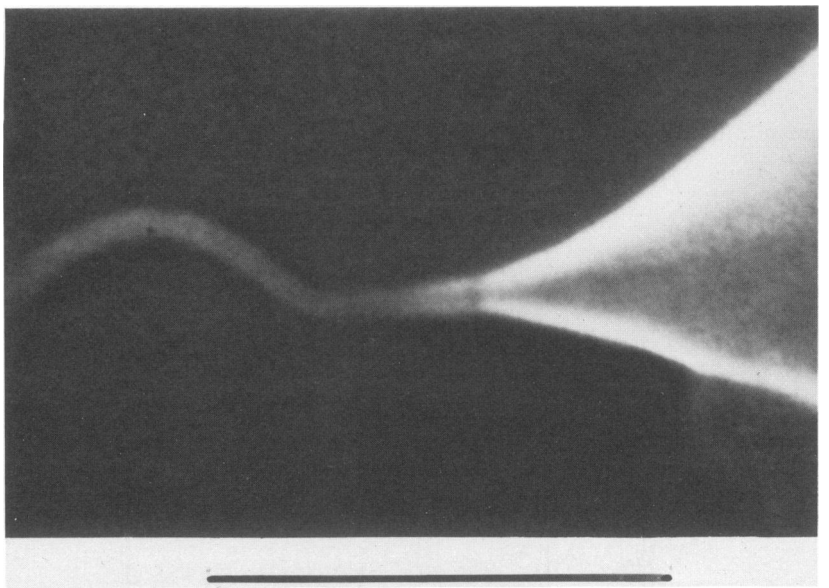

FIGURE 2 Scanning electron micrograph of a glutaraldehyde "fixed" microtether pulled from the red cell membrane by extracellular fluid shear. Extracellular fluid flow is from left to right with the tether attachment point at the extreme left and a portion of the cell body shown at the right. The curvature in the tether is an artifact which occurs during the drying process. (Compare with Fig. 6 in Hochmuth et al., 1973). Scale indicates 2 μm.

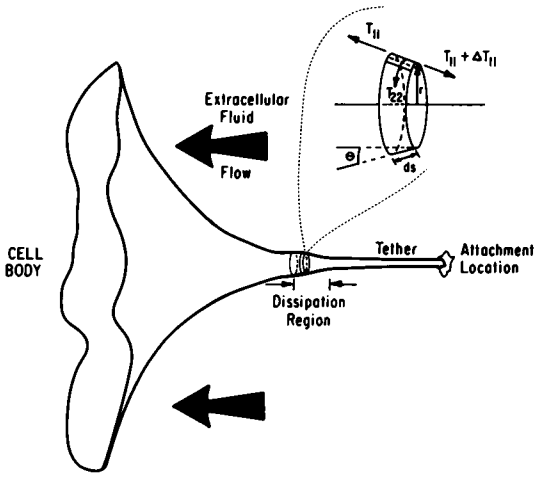

FIGURE 3 Schematic illustration of the microtether and the region of viscous dissipation or "necking" region where the dynamics of the plastic flow are important. The geometry of a membrane material element is shown in the enlarged view.

assumptions are made concerning the flow process. The advantage of the microtether experiment is that the growth primarily involves membrane flow with a minimum of cytoplasmic movement. This implies that the transmembrane, hydrostatic pressure can be neglected. The normal force that results from tension along the meridian (generator of the axially symmetric tether) is balanced by the tension in the circumferential direction ("hoop" tension). Therefore, a membrane material element is taken as a segment of a latitude ring formed by the surface between two planes normal to the tether axis. Fig. 3 illustrates the tether and element geometry.

The equations of equilibrium are determined by the balance of normal and tangential forces on the element (see Flügge, 1973).

$$(T_{11}/R_1) + (T_{22}/R_2) = 0,$$
$$(\mathrm{d}/\mathrm{d}s)(rT_{11}) - T_{22}(\mathrm{d}r/\mathrm{d}s) = 0, \tag{17}$$

where R_1, R_2 are the local principal radii of curvature of the membrane surface, and $\mathrm{d}s$, $\mathrm{d}r$ are incremental distances along the meridian and radius, respectively. The total force that acts on the cell body, created by the flowing extracellular fluid, is balanced by the projection of the tension, T_{11}, in the axial direction times the local circumference.

$$2\pi r \cos\theta\, T_{11} = F_s, \tag{18}$$

where r is the local radius and θ is the angle between the meridian and the tether axis. The force, F_s, is given by the surface area of the cell exposed to the fluid shear and the shear stress, τ_s, produced by the extracellular fluid:

$$F_s = \tau_s A. \tag{19}$$

Using Eq. 18 and either one of Eq. 17 (because the other will be identically satisfied) specifies the balance of forces on the material element and the principal membrane tensions.

$$T_{11} = F_s/2\pi r\cos\theta,$$
$$r(\mathrm{d}T_{11}/\mathrm{d}s) + (T_{11} - T_{22})(\mathrm{d}r/\mathrm{d}s) = 0. \tag{20}$$

Now, the plastic flow of membrane material from the cell to the tether can be determined using the constitutive relation between shear resultant and the rate of deformation given by either Eq. 15 or 16. In conjunction with the relationship between rate of deformation and shear resultant, it is necessary to establish the character of the initial boundary that is the intersection between the microtether and the cell body. At this location, the extrusion process begins. Upstream (in the cell body membrane), the fluid shear forces are balanced by the elastic deformation of the membrane (Evans, 1973*b*). Downstream (in the tether membrane), the forces are resisted by the rate of deformation of the membrane forming the tether (Eq. 15 or 16). Because we *assume* that the membrane shear-resultant is equal to the yield shear just upstream of the intersection, no membrane flow can occur unless the shape is in the form of a cylinder (for axial motion of a cylindrical surface, the rate of deformation is zero). Therefore, in the vicinity of the yield point (at the tether intersection with the cell body), the boundary condition is that the membrane forms a cylindrical surface and, therefore, $\theta \equiv 0$.[2] To produce yield and plastic deformation, the membrane shear resultant must exceed the yield shear; this occurs by changing the angle θ of the surface relative to the tether axis. As shown in Fig. 3, the angle is zero at the intersection with cell body and progressively increases as the region of dissipation is entered (after plastic flow commences). With increased tether growth, additional membrane material is pulled from the cell body. The tether radius decreases as the plastic extension continues until a minimum cross section is attained, determined by the finite thickness of the membrane itself. Any element that reaches the minimum radius condition becomes a fixed cylinder and no further rate of deformation can occur in the element. Therefore, there will be a finite region between these two cylinders where viscous dissipation occurs. (The minimum tether radius will be determined by the structural matrix that is involved in the plastic flow process. As we will show, the lipid bilayer, which probably lies superficially over the matrix, offers negligible resistance to the material shear. However, the effect of the tether radius on area compressibility of each lipid layer may contribute to a normal traction and resistance to decreasing the tether radius. The structural matrix may also include a small amount of cytoplasmic fluid that has formed a gel with the

[2] In general, viscous dissipation also occurs in the cell body as material moves along the surface with complete capability of elastic recovery. Such viscoelastic behavior can be incorporated into the boundary condition by introducing specific conical angles, $\theta_0 > 0$, and the condition that the surface viscosity η_p in plastic flow equals the surface viscosity η_e for viscoelasticity at the tether intersection. However, as a first approximation (because the correction is related to $1 - \cos\theta_0$ which is small for small angles), we are analyzing the $\theta_0 = 0$ case.

matrix and will act to increase the minimum tether radius. It is important to recognize that the parameter, r_t, which is used in the plastic flow analysis is the radius of a cylindrical surface representing only the structural matrix. For a protein matrix under the lipid bilayer, the minimum radius, r_t, is the total tether radius minus the bilayer thickness.)

In order to obtain a relationship between the viscoplastic material properties (surface viscosity, η_p, and yield shear, T_0) and the experimentally determined variables (extracellular fluid shear stress, τ_s, tether growth rate, $\Delta L/\Delta t$, and minimum tether diameter, $2r_t$), the steady flow of membrane material through the region of dissipation is analyzed using Eulerian variables represented by Eq. 16:

$$2\eta_p(\mathrm{d}v_s/\mathrm{d}s) = (T_{11}/2) - (T_{22}/2) - T_0. \tag{21}$$

Eq. 16 has been rewritten in terms of the velocity component along the tether meridian (generator) and the corresponding coordinate. If the time rate of change of the length of a membrane element were to be considered (e.g. in the case of oscillating flow), then the Lagrangian variables represented in Eq. 15 would be more useful.

With the use of Eqs. 20 and 21, the tether flow relation is written as

$$(2\eta_p/T_0)(\mathrm{d}v_s/\mathrm{d}s) = -(F_s/4\pi T_0)\, r(\mathrm{d}/\mathrm{d}r)(1/r\cos\theta) - 1. \tag{22}$$

The continuity relation for the velocity along the tether generator (v_s) is used to obtain an alternate form for the rate of deformation:

$$(\mathrm{d}/\mathrm{d}s)(rv_s) = 0, \tag{23}$$

or,

$$(\mathrm{d}v_s/\mathrm{d}s) = (v_s/r)\sin\theta. \tag{24}$$

In terms of the initial velocity, v_{s_0}, and initial radius, r_0, Eq. 24 becomes

$$\mathrm{d}v_s/\mathrm{d}s = v_{s_0} r_0/r^2 \sin\theta,$$

and Eq. 22 can be written as

$$(t_0 v_{s_0} r_0/r^3)\sin\theta = -(\mathrm{d}/\mathrm{d}r)[(\tilde{F}/r\cos\theta) + \ln r], \tag{25}$$

where $\tilde{F} \equiv F_s/4\pi T_0$ and $t_0 \equiv 2\eta_p/T_0$, which is a characteristic time constant for the membrane material indicative of membrane "fluidity" (i.e., large values of t_0 correspond to more liquid-like behavior than small values of t_0).[3]

There is a critical (minimum) value of extracellular fluid shear stress, τ_s^{crit}, that must be exceeded in order to produce tether growth. Since Eq. 17 indicates that $T_{22} = 0$ in the cylindrical portion of the cell membrane just before yield, Eqs. 18, 19, and 21 establish an expression for the yield shear for a tether with minimum radius r_t:

$$\tau_s^{\mathrm{crit}} A = 4\pi r_t T_0. \tag{26}$$

[3] For an ideal solid, $t_0 = 0$ and for an ideal liquid, $t_0 \to \infty$.

As previously discussed, the membrane shear resultant equals the yield shear at the intersection of the tether with the cell body.

$$T_{11}(0)/2 = T_0. \tag{27}$$

From Eqs. 19, 20, 26, and 27, the parameter $\tilde{F}$ is found to equal the initial radius and,

$$\tilde{F} = F_s/4\pi T_0 = r_0 = (\tau_s/\tau_s^{crit})\, r_t. \tag{28}$$

Eq. 28 demonstrates that the initial radius, r_0, is related to the applied force-ratio, $\tau_s A/\tau_s^{crit} A$,

$$r_0/r_t = \tau_s/\tau_s^{crit} = \bar{\lambda}, \tag{29}$$

where λ is the maximum extension ratio for a material element (after yield has occurred).

The initial velocity, v_{s_0}, is relative to the dissipation region. The rate of tether growth, $\Delta L/\Delta t$, is measured between the attachment point and the cell body and will, therefore, equal the difference between the initial (upstream) and final (downstream) velocities, v_{s_0} and v_{s_t}, in the dissipation region:

$$\Delta L/\Delta t = v_{s_t} - v_{s_0}. \tag{30}$$

By Eq. 23 for continuity, $v_{s_t} = v_{s_0}\bar{\lambda}$ and Eq. 30 can be rewritten as

$$\Delta L/\Delta t = v_{s_0}(\bar{\lambda} - 1) = v_{s_t}(1 - 1/\bar{\lambda}), \tag{31}$$

It is apparent that v_{s_t} minus v_{s_0} is given in terms of experimentally measurable quantities and that when the extracellular fluid shear stress equals τ_s^{crit}, no growth will take place.

Eq. 25 can be written in dimensionless form:

$$(t_0 v_{s_t}/r_t)(\sin\theta/\tilde{r}^3) = -(\mathrm{d}/\mathrm{d}\tilde{r})[(\bar{\lambda}/\tilde{r}\cos\theta) + \ln\tilde{r}], \tag{32}$$

where a scaled radius, $\tilde{r}$, has been introduced that ranges between one and the maximum extension ratio, $\bar{\lambda}$. Eq. 32 is a nonlinear differential equation that specifies the surface angle, θ, as a function of radius and can only be solved on a digital computer. Eq. 32 is subject to the condition that $\theta = 0$ ($\mathrm{d}v_s/\mathrm{d}s = 0$) at the beginning and ending of the dissipation region where the curvature along the meridian goes to zero. Given these conditions, there is a specific relationship between the "flow constant", $t_0 v_{s_t}/r_t$, and the maximum extension ratio (shear stress ratio, τ_s/τ_s^{crit}). The value of the flow constant for a specific stress ratio is found by iterative numerical integration of Eq. 32 from the minimum radius to the maximum radius until the condition, $\cos\theta = 1$, is reached at the upstream end of the tether.

Fig. 4 is a plot of the dimensionless tether growth rate,

$$G_t \equiv (t_0/r_t)(\Delta L/\Delta t) = (t_0 v_{s_t}/r_t)[1 - (\tau_s^{crit}/\tau_s)], \tag{33}$$

as a function of extracellular fluid shear stress ratio, τ_s/τ_s^{crit}. Fig. 5 shows the geome-

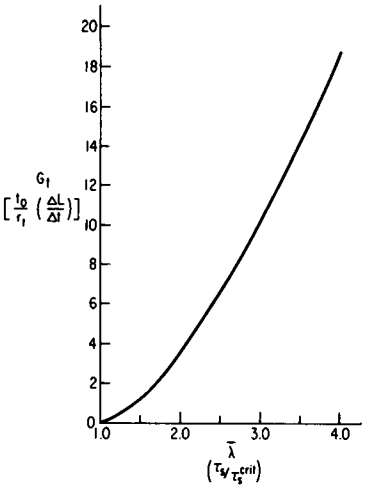

FIGURE 4

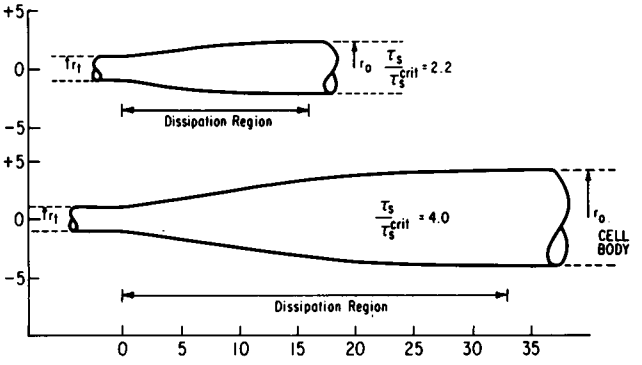

FIGURE 5

FIGURE 4 Plot of the dimensionless tether growth rate, $(t_0/r_t)(\Delta L/\Delta t)$, as a function of the extracellular fluid shear stress ratio, τ_s/τ_s^{crit}.

FIGURE 5 Calculated geometries for the region of dissipation are shown for two extracellular fluid shear stress ratios, $\tau_s/\tau_s^{crit} = 2.2$ and 4.

try of the dissipation region for two values of the fluid shear stress ratio, $\tau_s/\tau_s^{crit} = 2.2$, 4.

RED CELL MEMBRANE VISCO-PLASTIC PARAMETERS

In summary, the material properties of the membrane (the yield shear T_0 and the membrane viscosity η_p) that characterize its viscoplastic flow can be determined by,

$$T_0 = \tau_s^{crit} A/4\pi r_t (\text{dyn/cm}) \tag{34}$$

$$t_0 = r_t G_t/(\Delta L/\Delta t)(\text{seconds}) \tag{35}$$

$$\eta_p = T_0 t_0/2 (\text{dyn-s/cm}). \tag{36}$$

Therefore, it is necessary to know the total force on the tether (e.g., the extracellular fluid shear stress times the exposed surface area, $\tau_s A$), the minimum tether radius, r_t, the tether growth rate, $\Delta L/\Delta t$, and the minimum or "critical" force required to produce the tether (e.g., $\tau_s^{crit} A$).

Hochmuth et al. (1973) have published data on tether growth rate and the critical stress for tethering:

$$\tau_s^{crit} \approx 1.5 \text{ dyn/cm}^2$$

$$3 \times 10^{-6} \text{ cm/s} \leq \Delta L/\Delta t \leq 2 \times 10^{-5} \text{ cm/s}$$

for

$$1.3 \leq \tau_s/\tau_s^{crit} \leq 2.3.$$

Using the value of 70×10^{-8} cm^2 for the surface area exposed to extracellular fluid shear stress (one-half of the total red cell surface area), the yield shear is obtained in terms of the minimum tether radius from Eq. 34,

$$T_0 \approx (8 \times 10^{-8})/r_t(\text{cm})\,(\text{dyn/cm}).$$

The characteristic time constant, t_0, is obtained from Eq. 35, Fig. 4, and the data range taken from Hochmuth et al. (1973),

$$t_0 = r_t[0.7/(3 \times 10^{-6})] = r_t(\text{cm}) \cdot 2.3 \times 10^5\,(\text{seconds}),$$

or

$$t_0 = r_t[4.9/(2 \times 10^{-5})] = r_t(\text{cm}) \cdot 2.4 \times 10^5\,(\text{seconds}).$$

It is interesting to note that the ratio, $G_t/(\Delta L/\Delta t)$, which is proportional to the characteristic time constant, is essentially constant for the range of parameters given. The surface viscosity is calculated using Eq. 36, and the two previous relations (independent of the minimum tether radius),

$$\eta_p = 1 \times 10^{-2}\,\text{dyn-s/cm}.$$

In the companion article on membrane viscoelasticity, it is shown that the viscosity parameter, η_e, is of the order 10^{-3} dyn-s/cm when the membrane behaves in an elastic solid manner. As we have shown,[4] the surface viscosity determined from "fluidity" measurements of the lipid membrane components (Edidin, 1974*a* and *b*) is of the order 10^{-5} dyn-s/cm. It is apparent that the lipid bilayer contributes negligibly to the fluid dynamic resistance of the whole plasma membrane and that an additional structural matrix must be responsible for the observed mechanical behavior.

The minimum tether radius needs to be determined from scanning electron microscopy of red cells fixed in the sheared state. However, taking a range of 100–500 $\times$ 10^{-8} cm for the minimum radius of the plasma membrane (including sub-surface protein elements) will give a range for the yield shear of

$$1.6 \times 10^{-2}\,\text{dyn/cm} \leq T_0 \leq 8 \times 10^{-2}\,\text{dyn/cm}$$

and for the characteristic time constant of

$$0.2\,\text{s} < t_0 < 1.0\,\text{s}.$$

The red cell membrane exhibits hyperelastic behavior below the yield shear that can be modeled by a relationship between tension and extension ratio (Evans, 1973*b*),

$$T_{11} = (\mu/2)(\lambda_1^2 - \lambda_1^{-2}),$$

for the uniaxial extension of a material element at constant area. The two-dimensional

[4]Evans, E. A., and R. M. Hochmuth. Calculations of surface viscosity from lateral diffusion in membranes. Submitted for publication.

shear modulus, μ, has been measured at 7×10^{-3} dyn/cm (Evans and LaCelle, 1975). If it is assumed the membrane is perfectly elastic up to the yield shear, then the maximum *elastic* extension ratio an element can attain is given by

$$T_{11}/2 = T_0 = (\mu/4)(\lambda_E^2 - \lambda_E^{-2}).$$

For the range of yield shear given, the maximum elastic extension ratio would lie between

$$3 < \lambda_E < 6.$$

Evans and LaCelle reported that departure from elastic behavior appeared rapidly for extension ratios greater than 3:1 in micropipette aspiration experiments.

From the value of the yield shear, it is apparent that plastic (extension) failure of the membrane can occur at significantly lower tensions than in lysis (isotropic tensions of the order 5–20 dyn/cm, see Rand, 1964). The mechanisms of failure in isotropic tension (lysis) and in extension (plastic fragmentation) are different and need to be considered separately (Evans, 1975).

We thank Allen Rakow, research associate in Chemical Engineering at Washington University, for fixing the cells in glutaraldehyde and furnishing the photograph in Fig. 2.

Both authors are supported by U.S. Public Health Service NIH Research Career Development Awards, HL00063 and HL70612. In addition, this work was supported in part by USPHS NIH Grant HL16711 and National Science Foundation Grant GK43118.

Received for publication 25 April 1975.

REFERENCES

BESSIS, M. 1973. Living Blood Cells and Their Ultrastructure. Springer-Verlag, New York.

BULL, B. S., and I. N. KUHN. 1970. The production of schistocytes by fibrin strands. *Blood.* **35**:104.

BULL, B. S., M. L. RUBENBERG, J. V. DACIE, and M. C. BRAIN. 1968. Microangiopathic haemolytic anemia: mechanism of red-cell fragmentation. In vitro studies. *Br. J. Haematol.* **14**:643.

EDIDIN, M. 1974 *a*. Two-dimensional diffusion in membranes. *Symp. Soc. Exp. Biol.* **28**:1.

EDIDIN, M. 1974 *b*. Rotational and translational diffusion in membranes. *Ann. Rev. Biophys. Bioengr.* **3**:179.

EVANS, E. A. 1973 *a*. A new material concept for the red cell membrane. *Biophys. J.* **13**:926.

EVANS, E. A. 1973 *b*. New membrane concept applied to the analysis of fluid shear- and micropipette-deformed red blood cells. *Biophys. J.* **13**:941.

EVANS, E. A. 1975. Composite material structure of red cell membranes. *In* Erythrocyte Structure and Function. G. J. Brewer, editor. Alan Liss, New York. 491.

EVANS, E. A., and R. M. HOCHMUTH. 1976. Membrane viscoelasticity. *Biophys. J.* **16**:1.

EVANS, E. A., and P. L. LACELLE. 1975. Intrinsic material properties of the erythrocyte membrane indicated by mechanical analysis of deformation. *Blood.* **45**:29.

FLÜGGE, W. 1973. Stresses in Shells. Springer-Verlag, New York.

HOCHMUTH, R. M., and N. MOHANDAS. 1972. Uniaxial loading of the red cell membrane. *J. Biomech.* **5**:501.

HOCHMUTH, R. M., N. MOHANDAS, and P. L. BLACKSHEAR, JR. 1973. Measurement of the elastic modulus for red cell membrane using a fluid mechanical technique. *Biophys. J.* **13**:747.

KOCHEN, J. A. 1968. Visco-elastic properties of the red cell membrane. *In* Hemorheology. A. L. Copeley, editor. Pergamon Press, Oxford. 455.

LACELLE, P. L. 1970. Alteration of membrane deformability in hemolytic anemias. *Semin. Hematol.* **7**:355.

PRAGER, W. 1961. Introduction to Mechanics of Continua. Dover Publications, Inc. New York.

RAND, R. P. 1964. Mechanical properties of the red cell membrane. II. Viscoelastic breakdown of the membrane. *Biophys. J.* **4**:303.

SINGER, S. J., and G. L. NICOLSON. 1972. The fluid mosaic model of the structure of cell membranes. *Science (Washington, D.C.).* **175**:720.

SKALAK, R., A. TOZEREN, R. P. ZARDA, and S. CHIEN. 1973. Strain energy function of red blood cell membranes. *Biophys. J.* **13**:245.

WEED, R. I., and C. J. REED. 1965. The relation of erythrocyte fragmentation to cellular destruction. *Blood.* **26**:894.

WILLIAMSON, J. W., M. O. SHANAHAN, and R. M. HOCHMUTH. 1975. The influence of temperature on red cell deformability. *Blood.* In press.